Pharmaceutical Sciences and Drug Design
ISSN: 3062-4428
2025, Volume 5, Page No: 181-195

Available online at: www.galaxypub.co/page/journals

Galaxy Publication

Sodium Cantharidinate Enhances Cisplatin Sensitivity in Cervical Cancer via PTPN1-Mediated Inhibition of the PI3K/AKT Pathway

Sara Lindholm[1]*, Karin Berg[1]

[1]Department of Biotechnology, Faculty of Science, Lund University, Lund, Sweden.

***E-mail** ✉ sara.lindholm.se@outlook.com

Received: 21 April 2025; **Revised:** 26 August 2025; **Accepted:** 01 September 2025

ABSTRACT

Sodium cantharidinate (SC) has demonstrated efficacy in treating lung cancer in China, yet its effects in cervical cancer (CC)—a major cause of female reproductive cancer mortality—remain largely unexplored. This study investigates SC's anti-cancer activity in CC and explores the molecular mechanisms involved. DDP-resistant Caski-1 and ME180 cervical cancer cell lines were established and treated with SC to assess its impact on cell proliferation. Potential molecular targets of SC were predicted using bioinformatics analyses. Associations between PTPN1 expression and clinical features, including tumor stage, lymph node metastasis, and tumor differentiation, were evaluated. Functional studies included overexpressing PTPN1 in CC cells followed by treatment with SC and cisplatin. Additionally, the influence of SC on PI3K/AKT signaling and its effects on tumor growth and cisplatin resistance were assessed in vivo. SC treatment increased the responsiveness of Caski-1 and ME180 cells to cisplatin, augmenting its inhibitory effect on cell growth. Bioinformatic predictions suggested PTPN1 as a key SC target. Clinically, higher PTPN1 levels were correlated with advanced disease stage, lymph node involvement, and poor differentiation. SC suppressed PTPN1 expression, and PTPN1 overexpression reduced SC's anti-proliferative effects. Mechanistically, PTPN1 activated the PI3K/AKT pathway, which was inhibited by SC. In animal models, SC limited tumor growth and reversed cisplatin resistance. SC sensitizes cervical cancer cells to cisplatin by downregulating PTPN1 and inhibiting the PI3K/AKT pathway, highlighting its potential as a complementary therapeutic strategy.

Keywords: Cervical cancer, Sodium cantharidinate, Cisplatin, PTPN1, PI3K/AKT pathway

How to Cite This Article: Lindholm S, Berg K. Sodium Cantharidinate Enhances Cisplatin Sensitivity in Cervical Cancer via PTPN1-Mediated Inhibition of the PI3K/AKT Pathway. Pharm Sci Drug Des. 2025;5:181-95. https://doi.org/10.51847/1hgEHTNB9j

Introduction

Cervical cancer (CC) remains a leading cause of cancer-related death among women worldwide, accounting for a significant portion of both new cases and fatalities in 2018 [1]. While preventive measures such as vaccination and screening programs have improved early detection, many patients are still diagnosed at advanced stages or experience tumor recurrence. For these cases, systemic chemotherapy is often the primary therapeutic strategy [2]. Cisplatin (DDP), a platinum-based compound, is widely used due to its potent cytotoxic effects. Initially identified for its bacterial growth inhibition, DDP was later discovered to induce tumor cell death [3]. Nevertheless, the emergence of chemoresistance frequently undermines its efficacy in advanced CC, emphasizing the need to understand the molecular mechanisms controlling CC cell sensitivity to DDP [4].

Cantharidin, a bioactive terpenoid isolated from blister beetles, has demonstrated anti-cancer properties through mechanisms such as enzyme inhibition and cell cycle disruption [5]. It acts as a selective inhibitor of protein phosphatases 1 and 2A, modulating cell cycle progression and promoting apoptosis [6]. Sodium cantharidinate (SC), a water-soluble derivative of cantharidin, has been shown to trigger autophagic cell death in liver cancer models via LC3-dependent pathways [7]. However, its potential effects in CC remain largely unexplored.

Protein tyrosine phosphatases (PTPs) are critical regulators of cellular signaling, controlling processes like proliferation, survival, and differentiation through dephosphorylation of tyrosine residues [8]. Dysregulation of

these enzymes is implicated in various pathologies, including cancer [9]. PTPN1 (also known as PTP1B) has been identified as overexpressed in several tumor types, such as esophageal carcinoma [10], non-small cell lung cancer [11], breast cancer [12], and gliomas [13], and has been associated with therapy resistance in lung adenocarcinoma [14]. Despite these findings, its role in cervical cancer remains unclear.

This study aims to investigate whether PTPN1 contributes to chemoresistance in CC and whether SC can modulate its expression. Protein and mRNA levels of PTPN1 in Caski-1 and ME180 cells were examined using Western blotting and RT-qPCR. The potential of SC to sensitize CC cells to DDP was also evaluated, providing insight into novel therapeutic approaches for improving patient outcomes.

Materials and Methods

Clinical sample collection

Tissue samples were obtained from 59 patients with CC at The First Affiliated Hospital of Anhui Medical University between 2016 and 2019. All participants provided written informed consent, and the study protocol was approved by the institutional ethics committee in accordance with the Declaration of Helsinki. Patients who had received chemotherapy or radiotherapy before surgery, or who had other major diseases, were excluded. Diagnosis was confirmed by at least two independent pathologists. Clinical staging and pathological classification were determined using FIGO guidelines. Tissue samples were collected during surgery and immediately stored in liquid nitrogen for further analysis.

Generation of cisplatin-resistant cell lines

Caski-1 (#CDC0111) and ME180 (#HTB-33) cells were exposed to progressively increasing concentrations of DDP (#P4394, Sigma-Aldrich) to establish resistant variants. The initial exposure began at 1.52 μM (IC80 for parental cells) for 48 hours per week. Drug concentration was gradually escalated over six months, reaching 15.20 μM. Resistant cell lines (Caski-1/R and ME180/R) were maintained with monthly DDP treatment and cultured drug-free for two weeks prior to experiments.

Cell viability assay

Cells were seeded at 5 × 10^3 cells/well in 96-well plates and treated with a range of DDP concentrations (0.001–100 nmol/mL) for 72 hours. Cell viability was measured using the CellTiter-Glo® luminescent assay, normalized to DMSO controls, and IC50 values were determined using GraphPad Prism.

EdU proliferation assay

To assess cell proliferation, EdU incorporation assays were performed. Cells were pretreated with SC for 24 hours and then incubated with DDP for an additional 24 hours. Cells were fixed in cold ethanol/acetic acid (2:1) for 10 minutes, permeabilized with PBS containing 1% Triton X-100, and DNA was denatured with 4 mM HCl at 37°C for 15 minutes. Following neutralization with 0.1 M sodium borate (pH 8.5), cells were incubated with 10 μM EdU (#900584, Sigma-Aldrich) for 6 hours and counterstained with DAPI (#D8417, Sigma-Aldrich). Fluorescence images were captured using an Axiovert 200 microscope (×100, Carl Zeiss).

Experimental methods

Colony formation assay

Cells were seeded at 1 × 10^3 per well in 12-well plates and allowed to attach overnight. Drugs were then applied, and cultures were maintained for 12 days with medium changes every three days. Colonies were fixed in methanol for 10 minutes and stained with 0.1% crystal violet for visualization. Images of colonies were captured for analysis.

Apoptosis analysis by flow cytometry

Cell apoptosis was measured using the Annexin V/PI apoptosis detection kit (#C1062, Beyotime). Cells (1 × 10^5) were resuspended in 100 μL binding buffer and incubated with 5 μL Annexin V-FITC and 5 μL PI for 15 minutes in the dark at room temperature. After adding 400 μL binding buffer, samples were analyzed within 1 hour on a flow cytometer. Annexin V-FITC and PI fluorescence were recorded at 530 nm and 585 nm, respectively, and results were quantified using FlowJo software (v7.6.1, BD Biosciences).

Hoechst 33258 nuclear staining

Apoptotic nuclear morphology was assessed using Hoechst 33258 (#C1017, Beyotime). Fixed cells (4% paraformaldehyde, 30 minutes, room temperature) were incubated with 5 μg/mL Hoechst 33258 for 20 minutes at 37°C in the dark. Fluorescent images were captured using a Nikon fluorescence microscope, and the proportion of apoptotic cells was semi-quantified using Image-Pro Plus 6.0 (Media Cybernetics).

Immunofluorescence analysis

Transfected cells were stained with primary antibodies against CD133 (ab216323, Abcam), CD44 (ab51037, Abcam), and SOX2 (MAB4423, Millipore). Alexa Fluor 488-conjugated secondary antibodies were applied, and nuclei were counterstained with coverslips (Invitrogen). Images were acquired using a confocal laser scanning microscope (Leica Microsystems), and fluorescence intensity was measured in five fields containing at least 300 cells per coverslip using ImageJ 1.37v.

Sphere formation assay

Caski-1/R and ME180/R cells were seeded at 1 × 10^3 cells/mL in ultra-low attachment 6-well plates. Cells were cultured in DMEM/F12 supplemented with EGF (20 ng/mL), bFGF (20 ng/mL), and B27 supplement. After 12 days, spheres were counted to assess self-renewal capacity.

Lactate dehydrogenase (LDH) cytotoxicity assay

Cells (1.5 × 10^5 per well) were plated in 24-well plates overnight. Culture supernatants were collected and transferred to 96-well plates (200 μL/well). LDH release was quantified using the LDH Cytotoxicity Assay Kit (#C0016, Beyotime) following manufacturer instructions, with absorbance measured at 450 nm.

Caspase-3 activity measurement

Cells were treated with SC or DDP for 72 hours. Caspase-3 activity was assessed using the Caspase-Glo 3 kit (#G8090, Promega) according to the manufacturer's protocol in 96-well plates.

RT-qPCR

Total RNA was extracted from cells or spheres using TRIzol reagent (Sigma-Aldrich). Reverse transcription was performed using 10 ng RNA with the TaqMan RNA RT kit (Applied Biosystems). Quantitative PCR was carried out in quadruplets on a Rotor-Gene Q 6000 system, and expression levels were analyzed using Rotor-Gene software. Primers were purchased from Exiqon (Cat. no. 204337).

Western blotting

Cells or tissue samples were lysed in RIPA buffer containing 1 mM sodium fluoride. Protein (20 μg) was separated by 8–12% SDS-PAGE and transferred to PVDF membranes (Millipore). Membranes were blocked in 5% skim milk for 90 minutes and incubated overnight at 4°C with primary antibodies against PTPN1 (MABS197, Millipore), phospho-PI3K (ab182651, Abcam), and phospho-AKT1 (#bs-1448R, Bioss). After washing, membranes were incubated with HRP-conjugated secondary antibodies (1:10,000; Proteintech) for 60 minutes at room temperature. Proteins were visualized using enhanced chemiluminescence (Beyotime).

Xenograft tumor model

All animal experiments were approved by the institutional animal care committee. Female nude mice (5 weeks old, 20–22 g, n=6 per group) were subcutaneously injected in the axilla with 3 × 10^6 Caski-1 or Caski-1/R cells. Mice were administered SC (100 mg/kg/day) or PBS via oral gavage, with DDP treatment every 5 days. Tumor volumes were measured every 5 days from day 5 post-injection using the formula: volume = (length × width^2)/2. Anesthesia was administered intravenously with pentobarbital sodium (100 mg/kg), and all efforts were made to minimize animal distress.

Immunohistochemistry (IHC)

Tumor tissue sections were incubated overnight at 4°C with primary antibodies against KI67 (1:400, #bs-2007R, Bioss), PTPN1 (1:500, MABS197, Millipore), phospho-PI3K (1:400, ab182651, Abcam), and phospho-AKT1

(1:400, #bs-1448R, Bioss). Sections were treated with HRP-conjugated secondary antibodies at 37°C for 60 minutes, developed with DAB, and left at room temperature for 10 minutes. Staining intensity and proportion of positive cells were scored using a semiquantitative system combining degree (0–4) and intensity (0–3), with the sum representing the final score.

TUNEL assay

Apoptotic cells in tissue sections were quantified using the TUNEL assay kit (#G7360, Promega). Paraffin-embedded sections were deparaffinized, rehydrated, and subjected to antigen retrieval with proteinase K. After permeabilization, slides were incubated at 37°C for 2 hours with a TdT/dUTP mixture (1:9). Endogenous peroxidase activity was subsequently blocked, and tissues were treated with converter-peroxidase reagent (Reagent 3), followed by DAB development. Nuclei were counterstained with hematoxylin for 3 minutes. Sections were dehydrated through a graded ethanol series (70%, 80%, 95%, 100%), cleared in xylene, and mounted with resin. Apoptotic nuclei appeared brownish-yellow, while hematoxylin-stained nuclei were blue. Slides were imaged and analyzed with Image-Pro Plus 6.0 (Media Cybernetics).

Statistical analysis

Experiments were performed in triplicate or more. Data were analyzed using SPSS 20.0 (IBM Corp., Armonk, NY, USA) and GraphPad Prism 8.0 (GraphPad Software, San Diego, CA, USA). Differences among groups were evaluated using one-way or two-way ANOVA followed by Tukey's multiple comparisons test or Student's t-test, as appropriate. Results are presented as mean ± standard deviation (SD), and statistical significance was defined as $p < 0.05$.

Results and Discussion

Establishment of DDP-resistant cervical cancer cell lines

To investigate mechanisms of cisplatin resistance, we gradually exposed Caski-1 and ME180 cells to increasing concentrations of DDP, ultimately generating resistant lines designated Caski-1/R and ME180/R. The successful establishment of these resistant cells was confirmed by evaluating their viability at different DDP concentrations using the CellTiter-Glo (CTG) assay. Resistant cells exhibited significantly higher IC50 values compared to parental cells **(Figure 1a)**.

Next, parental and resistant cells were treated with 10 μM DDP for 6 hours to assess apoptosis and proliferation. Flow cytometry revealed that parental cells underwent a higher rate of apoptosis, while EdU staining showed markedly reduced proliferation in these cells relative to their resistant counterparts **(Figures 1b and 1c)**.

We then examined the expression of stemness-associated markers CD133, CD44, and SOX2 via immunofluorescence. Resistant cells demonstrated notably elevated levels of all three markers **(Figure 1d)**. Furthermore, drug-resistant cells formed larger tumor spheres compared to parental cells, indicating enhanced self-renewal capacity **(Figure 1e).**

Collectively, these findings confirm the successful generation of DDP-resistant CC cell lines, which display stem cell-like characteristics, including increased marker expression and sphere-forming ability.

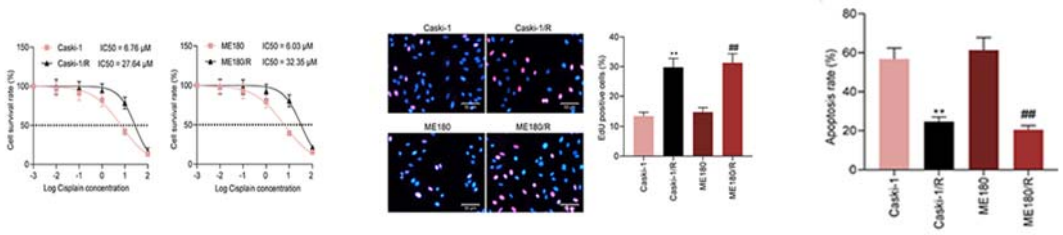

a) b) c)

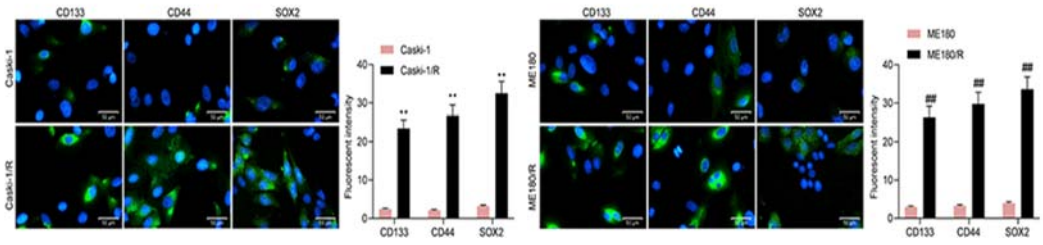

d)

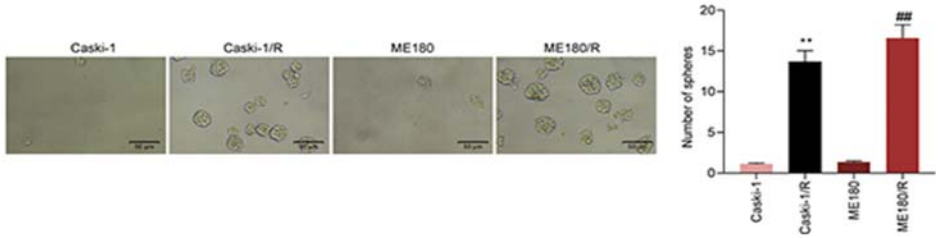

e)

Figure 1. Establishment of cisplatin-resistant cervical cancer cell models.
(a) Cellular viability measured with the CellTiter-Glo assay.
(b) Proliferative capacity analyzed via EdU labeling.
(c) Apoptotic populations quantified through flow cytometry.
(d) Stem cell-associated marker expression (CD133, CD44, SOX2) visualized using immunofluorescence.
(e) Evaluation of tumor sphere formation, including size and number.
Experiments were repeated at least three times. Values are presented as mean ± SD. Statistical differences were analyzed using one-way ANOVA (B, C, E) or two-way ANOVA (A, D) with Tukey's post hoc test. **p < 0.01 vs Caski-1 cells; ##p < 0.01 vs ME180 cells.

SC suppresses growth and stemness in cervical cancer cells

Given previous evidence that sodium cantharidinate (SC) induces apoptosis in hepatocellular carcinoma [7], we investigated whether SC exerts similar anti-proliferative effects in cervical cancer. Parental and cisplatin-resistant Caski-1 and ME180 cells were exposed to increasing SC concentrations, and viability was assessed. A concentration-dependent decrease in cell viability was observed across all lines, with higher SC doses causing greater reductions in survival **(Figures 2a and 2b)**. Concurrently, apoptosis was significantly elevated in treated cells compared with untreated controls **(Figure 2c)**.

To examine whether SC affects stem cell-like properties, we assessed the expression of CD133, CD44, and SOX2 in drug-resistant cells. Immunofluorescence revealed a marked downregulation of these markers following SC treatment **(Figure 2d)**. Moreover, sphere-forming ability was substantially impaired: both the number and diameter of spheres formed by Caski-1/R and ME180/R cells declined after SC exposure **(Figure 2e)**.

These data indicate that SC not only suppresses cell proliferation and triggers apoptosis but also diminishes the stemness features of both parental and cisplatin-resistant cervical cancer cells, suggesting its potential as an adjuvant therapy for overcoming drug resistance.

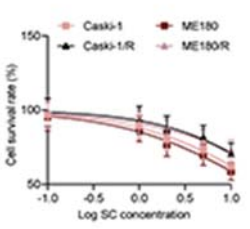

a)

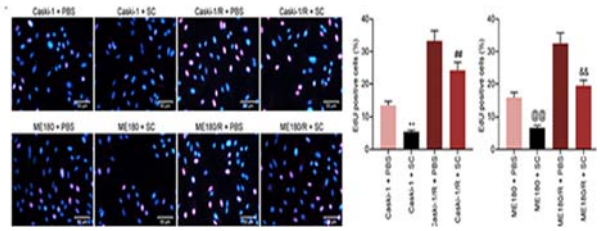

b)

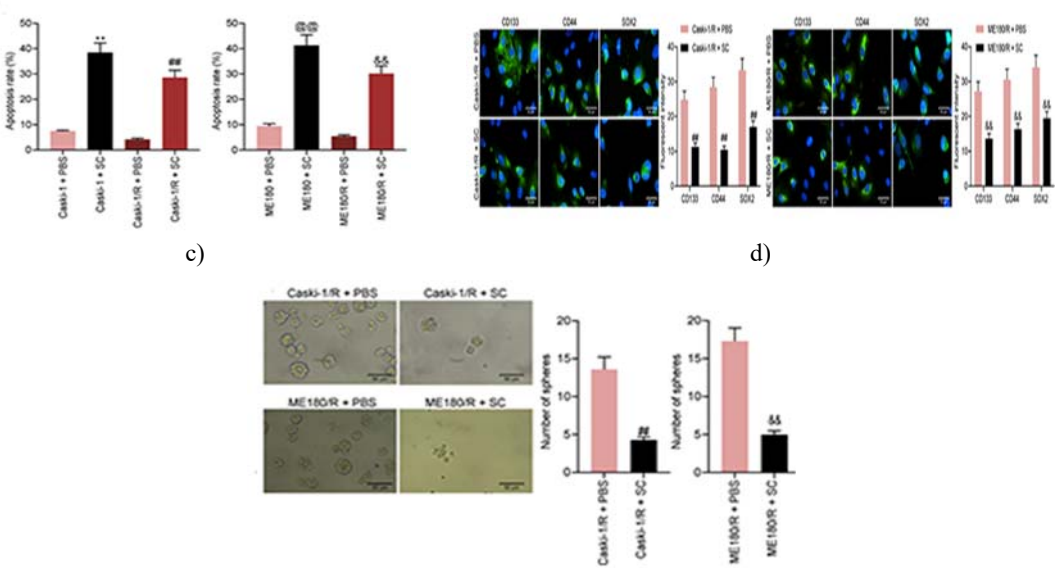

c) d)

e)

Figure 2. Effects of sodium cantharidinate (SC) on cervical cancer cells.
CC cells were exposed to SC alone.
(a) Viability of cells determined using the CellTiter-Glo assay.
(b) Proliferative capacity measured by EdU incorporation.
(c) Apoptosis rates quantified via flow cytometry.
(d) Expression of stemness-related markers (CD133, CD44, SOX2) evaluated by immunofluorescence.
(e) Sphere formation analyzed for size and quantity.
All experiments were independently repeated three times. Data are reported as mean ± SD. Statistical significance was calculated using unpaired t-test (panel E), one-way ANOVA (panels B, C), or two-way ANOVA (panels A, D) with Tukey's post hoc test. **p < 0.01 vs Caski-1 + PBS; ##p < 0.01 vs Caski-1/R + PBS; @@p < 0.01 vs ME180 + PBS; &&p < 0.01 vs ME180/R + PBS.

SC increases cisplatin sensitivity in cervical cancer cells

After demonstrating that SC can inhibit proliferation and reduce stem-like features in cervical cancer cells, we explored whether it can enhance cisplatin responsiveness. Parental and cisplatin-resistant Caski-1 and ME180 cells were pre-treated with 50 μM SC and then exposed to increasing concentrations of DDP to determine IC50 values. SC pre-treatment significantly lowered IC50 values in all cell lines, suggesting that SC increases the susceptibility of both parental and resistant cells to cisplatin **(Figure 3a)**.

Subsequent experiments revealed that combining SC with DDP strengthened growth inhibition compared with cisplatin alone **(Figures 3b and 3b)**. Apoptotic cell fractions were also higher following combination treatment, indicating enhanced pro-apoptotic effects **(Figures 3d and 3e).** To assess cytotoxicity, LDH release was measured and found to be elevated in cells receiving both SC and DDP **(Figure 3f)**. Additionally, caspase-3 activity assays confirmed a rise in apoptosis under combination therapy **(Figure 3g)**.

These findings collectively indicate that SC not only suppresses cell proliferation and stemness in cervical cancer cells but also potentiates the anti-tumor effects of cisplatin by promoting apoptosis and cytotoxicity in both parental and resistant cell populations.

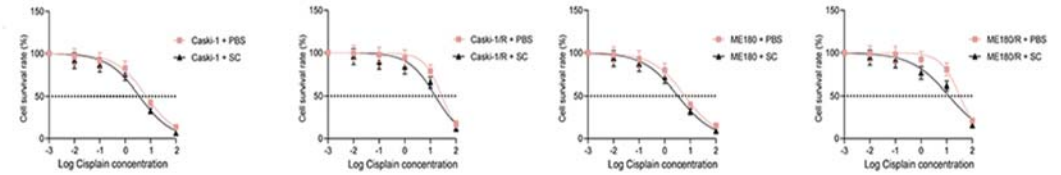

a)

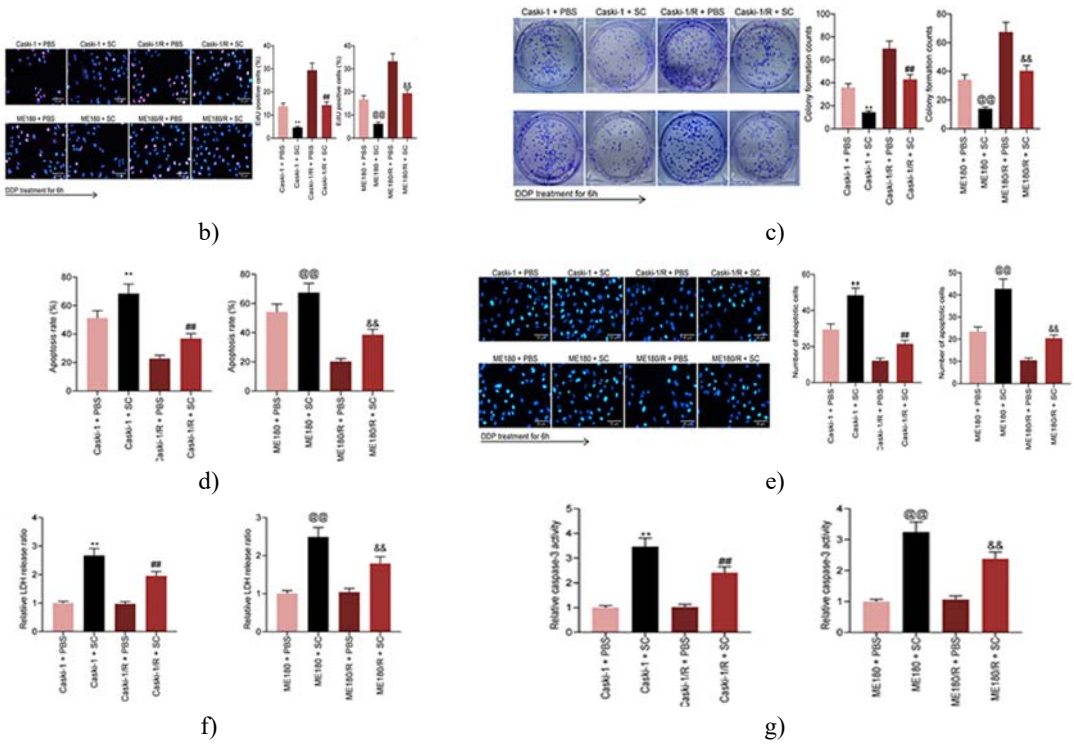

Figure 3. SC enhances the response of cervical cancer cells to cisplatin.
Caski-1 and ME180 cells, including their cisplatin-resistant variants, were treated with DDP in the presence of 50 μM SC.
(a) Viability of cells assessed using the CellTiter-Glo assay.
(b) EdU staining used to measure proliferative activity.
(c) Colony formation capacity evaluated over 10–12 days.
(d) Apoptosis quantified by flow cytometry.
(e) Hoechst 33258 staining employed to detect nuclear changes associated with apoptosis.
(f) Cytotoxicity measured by LDH release assay.
(g) Caspase-3 enzymatic activity determined to confirm apoptosis induction.
All experiments were repeated three times independently. Data are expressed as mean ± SD. Statistical significance was determined using one-way ANOVA (panels B–G) or two-way ANOVA (panel A) followed by Tukey's post hoc test. **p < 0.01 vs Caski-1 + PBS; ##p < 0.01 vs Caski-1/R + PBS; @@p < 0.01 vs ME180 + PBS; &&p < 0.01 vs ME180/R + PBS.

SC Enhances cisplatin efficacy by targeting PTPN1

To identify potential molecular targets of SC, we utilized the SWISS Target Prediction platform (http://www.swisstargetprediction.ch/). Analysis indicated that SC primarily interacts with phosphatase-related proteins, with PTPN1 emerging as a notable candidate **(Figures 4a and 4b).**

We next examined PTPN1 expression in parental and cisplatin-resistant Caski-1 and ME180 cells. DDP-resistant cells exhibited significantly higher levels of PTPN1 compared to their parental counterparts. Treatment with SC led to a pronounced reduction in PTPN1 expression in both cell lines **(Figures 4c and 4d)**.

To explore clinical relevance, we assessed PTPN1 expression in tumor tissues from 59 cervical cancer patients. Elevated PTPN1 was significantly associated with higher FIGO stage, increased likelihood of lymph node metastasis, and poorer differentiation. There was no notable correlation between PTPN1 levels and patient age or tumor size **(Table 1)**.

These findings suggest that the ability of SC to sensitize cervical cancer cells to cisplatin may be mediated, at least in part, through suppression of PTPN1, a phosphatase linked to tumor progression and chemoresistance.

Table 1. Correlation Analysis Between PTPN1 Expression and Clinical Features (N = 59)

Parameters	Total Cases	PTPN1 Expression Level		*p* value
		Low (n = 29)	High (n = 30)	
Age (years)				0.796
< 50	28	13	15	
> 50	31	16	15	
Tumor size (cm)				0.195
< 4	32	13	19	
> 4	27	16	11	
Depth of invasion				0.0673
< 2/3	25	16	9	
> 2/3	34	13	21	
FIGO stage				0.038
0–I	29	19	10	
IIa–IIIb	30	10	20	
Lymphatic metastasis				0.003
With	24	6	18	
Without	35	23	12	
Differentiated level				< 0.001
Poor	14	1	13	
Moderate + well	45	28	17	

Abbreviation: FIGO, International Federation of Gynecology and Obstetrics.

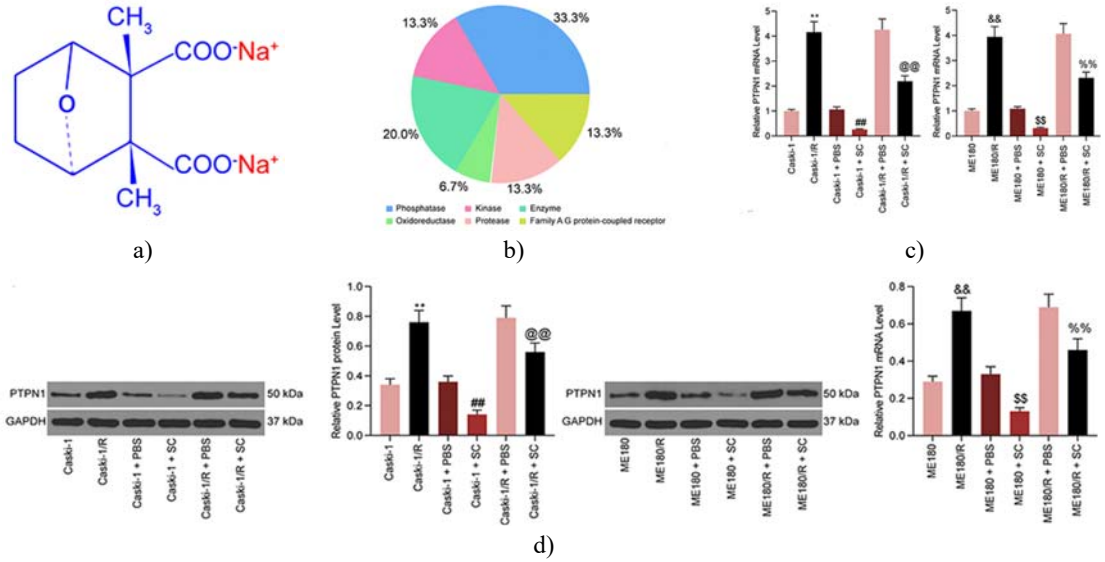

Figure 4. Targeting PTPN1 underlies SC-mediated enhancement of cisplatin efficacy in cervical cancer cells.
(a) Molecular structure of sodium cantharidinate (SC).
(b) Predicted protein targets of SC generated via the SWISS Target Prediction platform (http://www.swisstargetprediction.ch/).
(c) Quantification of PTPN1 mRNA levels in Caski-1 and ME180 cells using RT-qPCR.
(d) Western blot analysis showing PTPN1 protein levels in the same cells.
Experiments were repeated at least three times independently. Values are reported as mean ± SD. Statistical analysis was conducted using one-way ANOVA with Tukey's post hoc test. **p < 0.01 vs Caski-1; ##p < 0.01 vs Caski-1 + PBS; @@p < 0.01 vs Caski-1/R + PBS; &&p < 0.01 vs ME180; $$p < 0.01 vs ME180 + PBS; %%p < 0.01 vs ME180/R + PBS.

Overexpression of PTPN1 diminishes SC's sensitizing effect on cisplatin

To test whether SC enhances cisplatin sensitivity through PTPN1 suppression, PTPN1 was overexpressed in both parental and DDP-resistant Caski-1 and ME180 cells. Successful upregulation was confirmed at the mRNA and protein levels by RT-qPCR and Western blot, respectively **(Figures 5a and 5b)**.

Following PTPN1 overexpression, cells displayed higher IC50 values for cisplatin, indicating reduced responsiveness **(Figure 5c)**. Growth inhibition induced by the combination of SC and cisplatin was partially reversed **(Figures 5d and 5e)**, and the proportion of apoptotic cells was markedly decreased compared to vector controls **(Figure 5f)**.

Consistent with these results, SC-mediated increases in LDH release and caspase-3 activity were also suppressed in PTPN1-overexpressing cells **(Figures 5g and 5i)**. These observations indicate that PTPN1 plays a key role in mediating the enhanced cisplatin sensitivity caused by SC, and restoring its expression counteracts this effect.

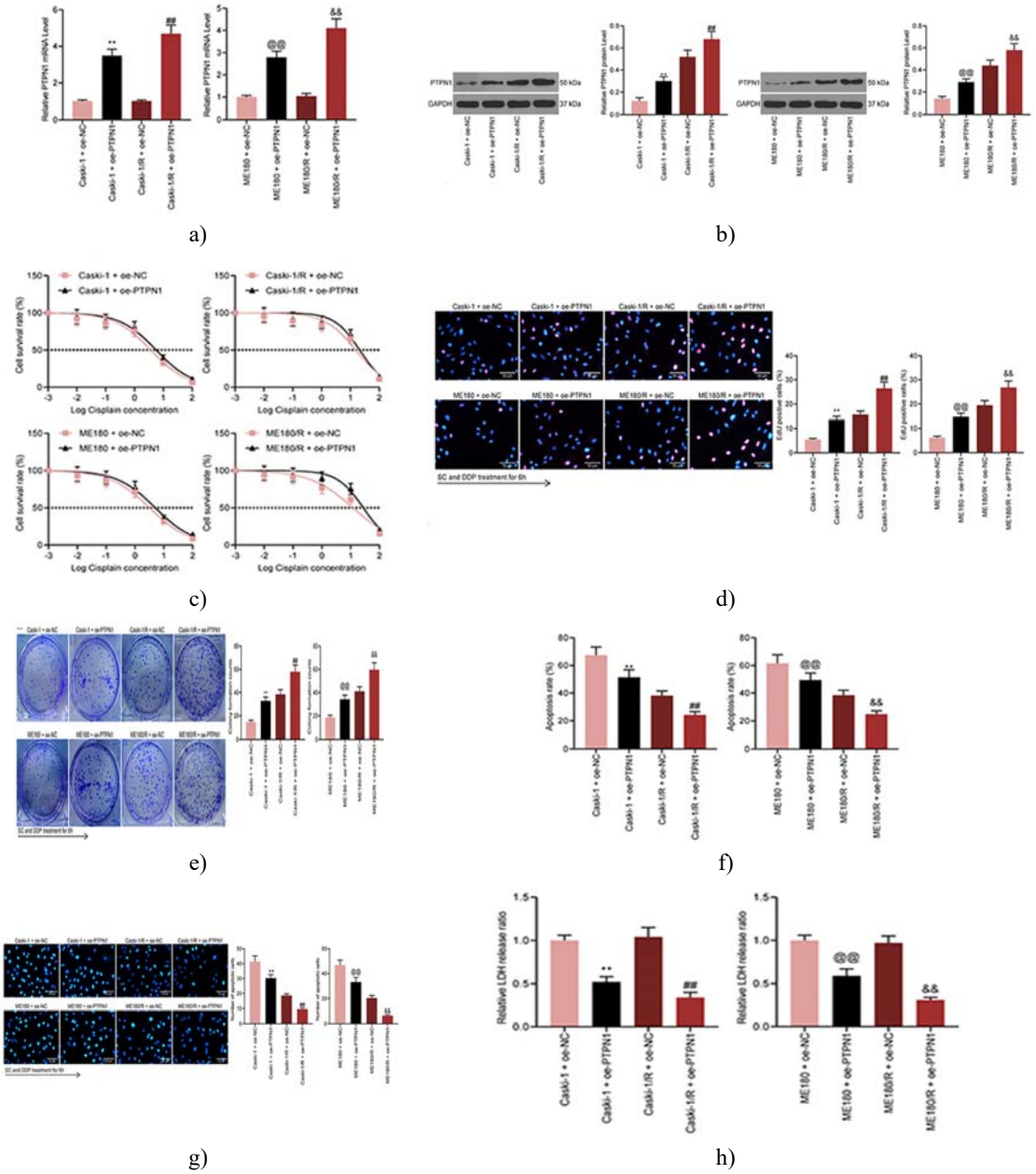

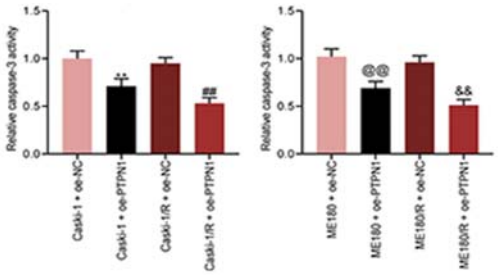

i)

Figure 5. PTPN1 overexpression reduces SC-induced enhancement of cisplatin cytotoxicity in cervical cancer cells.

Parental and cisplatin-resistant Caski-1 and ME180 cells were genetically modified to overexpress PTPN1, then exposed to SC and cisplatin.

(a) RT-qPCR analysis of PTPN1 transcript levels.

(b) Western blot evaluation of PTPN1 protein expression.

(c) Assessment of cell viability using the CellTiter-Glo assay.

(d) EdU incorporation assay showing proliferative capacity.

(e) Colony formation assay evaluating long-term growth potential.

(f) Flow cytometry quantification of apoptotic cells.

(g) Hoechst 33258 staining to detect nuclear changes associated with apoptosis.

(h) Measurement of LDH release as an indicator of cytotoxicity.

(i) Caspase-3 activity assay confirming apoptosis induction.

All experiments were repeated three or more times independently. Data are presented as mean ± SD. Statistical comparisons were conducted using one-way ANOVA (panels A, B, D–I) or two-way ANOVA (panel C) with Tukey's post hoc test. **p < 0.01 vs Caski-1 + oe-NC; ##p < 0.01 vs Caski-1/R + oe-NC; @@p < 0.01 vs ME180 + oe-NC; &&p < 0.01 vs ME180/R + oe-NC.

PTPN1 activates PI3K/AKT signaling to promote drug resistance (rewritten)

Previous studies have suggested that PTPN1 can enhance tumor aggressiveness by activating the PI3K/AKT signaling cascade [15]. To determine whether this pathway contributes to chemoresistance in cervical cancer, phosphorylation levels of PI3K and AKT were analyzed in both parental and cisplatin-resistant Caski-1 and ME180 cells. Resistant cells displayed markedly higher phosphorylation of these kinases compared to parental cells. SC treatment effectively reduced PI3K and AKT activation, but overexpression of PTPN1 partially restored their phosphorylation, indicating that SC exerts its effects at least in part via PTPN1 suppression (**Figures 6a and 6b).**

To further verify the role of PI3K/AKT, cells were treated with the pathway activator Recilisib in combination with SC. Reactivation of PI3K/AKT signaling increased cisplatin IC50 values in both sensitive and resistant cells, confirming that pathway activation diminishes drug efficacy **(Figure 6c)**. Additionally, Recilisib counteracted SC's ability to inhibit proliferation and induce apoptosis, demonstrating that SC's chemosensitizing effect relies on suppression of PI3K/AKT **(Figures 6d and 6h)**.

Overall, these results indicate that SC enhances cisplatin sensitivity in cervical cancer cells primarily by downregulating PTPN1 and thereby inhibiting the PI3K/AKT pathway.

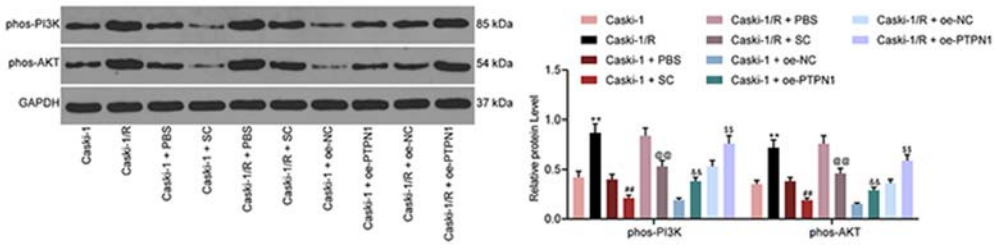

a)

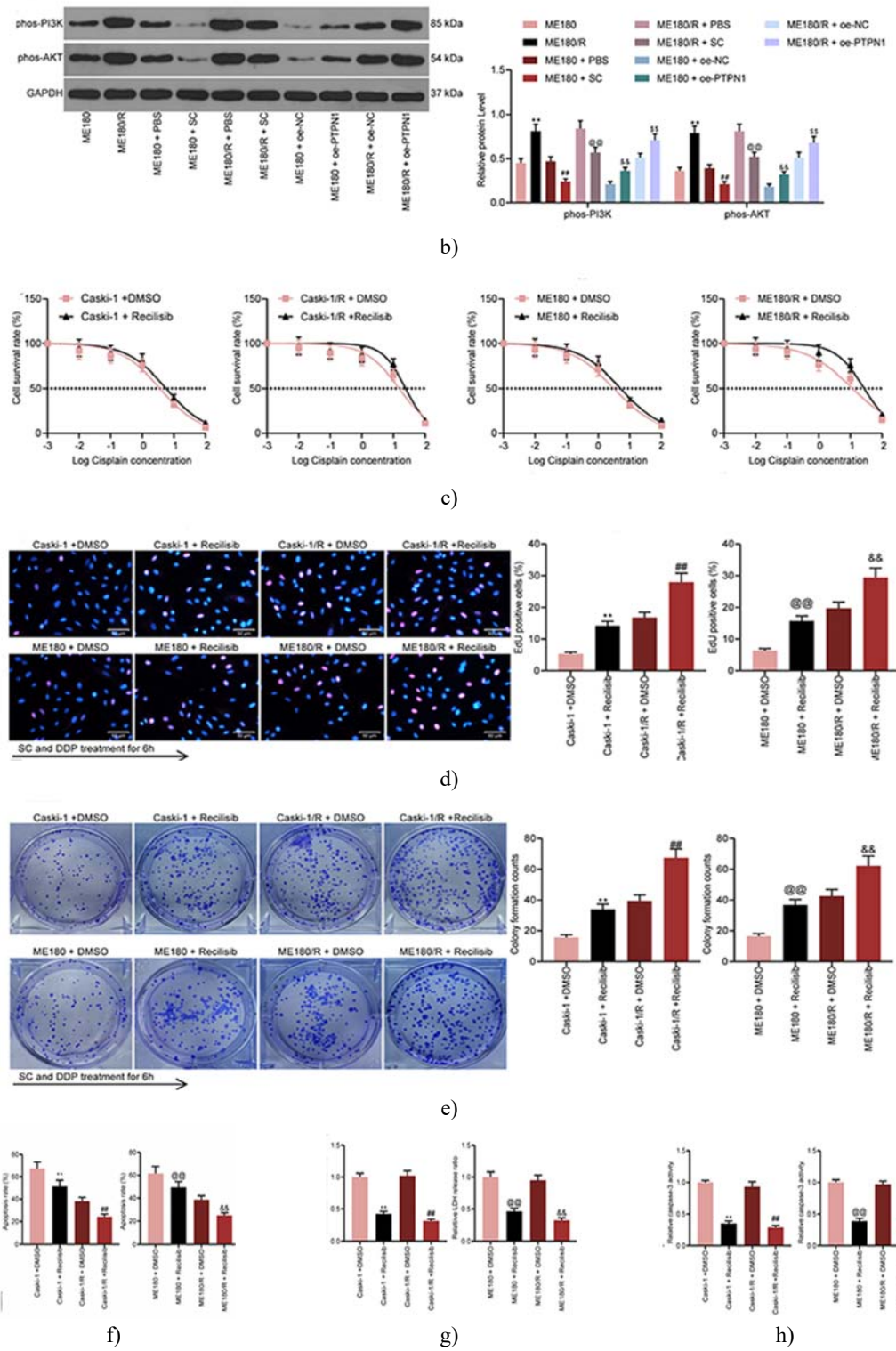

Figure 6. PTPN1 regulates PI3K/AKT signaling and affects cisplatin response in cervical cancer cells. (a) Western blot analysis showing phosphorylated PI3K and AKT in parental and cisplatin-resistant Caski-1 cells.

(b) Western blot analysis of phosphorylated PI3K and AKT in parental and resistant ME180 cells. To test whether PI3K/AKT signaling modulates SC's effect on drug response, cells were treated with the PI3K/AKT activator Recilisib alongside SC and cisplatin.

(c) Cell viability assessed by CellTiter-Glo assay.
(d) Proliferation measured through EdU incorporation.
(e) Long-term growth evaluated by colony formation.
(f) Apoptosis quantified by flow cytometry.
(g) LDH release as a marker of cytotoxicity.
(h) Caspase-3 activity as an indicator of apoptosis.
Data represent mean ± SD from three independent experiments. Statistical significance was calculated using one-way ANOVA (d–h) or two-way ANOVA (A–C) with Tukey's post hoc test.

SC Reduces tumor growth and chemoresistance in vivo

To examine the in vivo effects of SC, nude mice were subcutaneously implanted with either parental or cisplatin-resistant Caski-1 cells. SC (100 mg/kg/day) was administered by oral gavage, and cisplatin was given every five days. Tumor sizes were measured at five-day intervals starting on day 5. SC treatment significantly decreased tumor growth and overcame cisplatin resistance compared to controls **(Figures 7b and 7c)**.

Immunohistochemistry of tumor sections demonstrated marked reductions in KI67, PTPN1, and phosphorylated PI3K and AKT levels after SC treatment **(Figures 7d and 7g)**. Additionally, TUNEL assays showed a higher proportion of apoptotic cells in tumors treated with SC **(Figure 7h)**. Collectively, these results indicate that SC enhances cisplatin sensitivity by suppressing PTPN1 and dampening PI3K/AKT signaling in vivo.

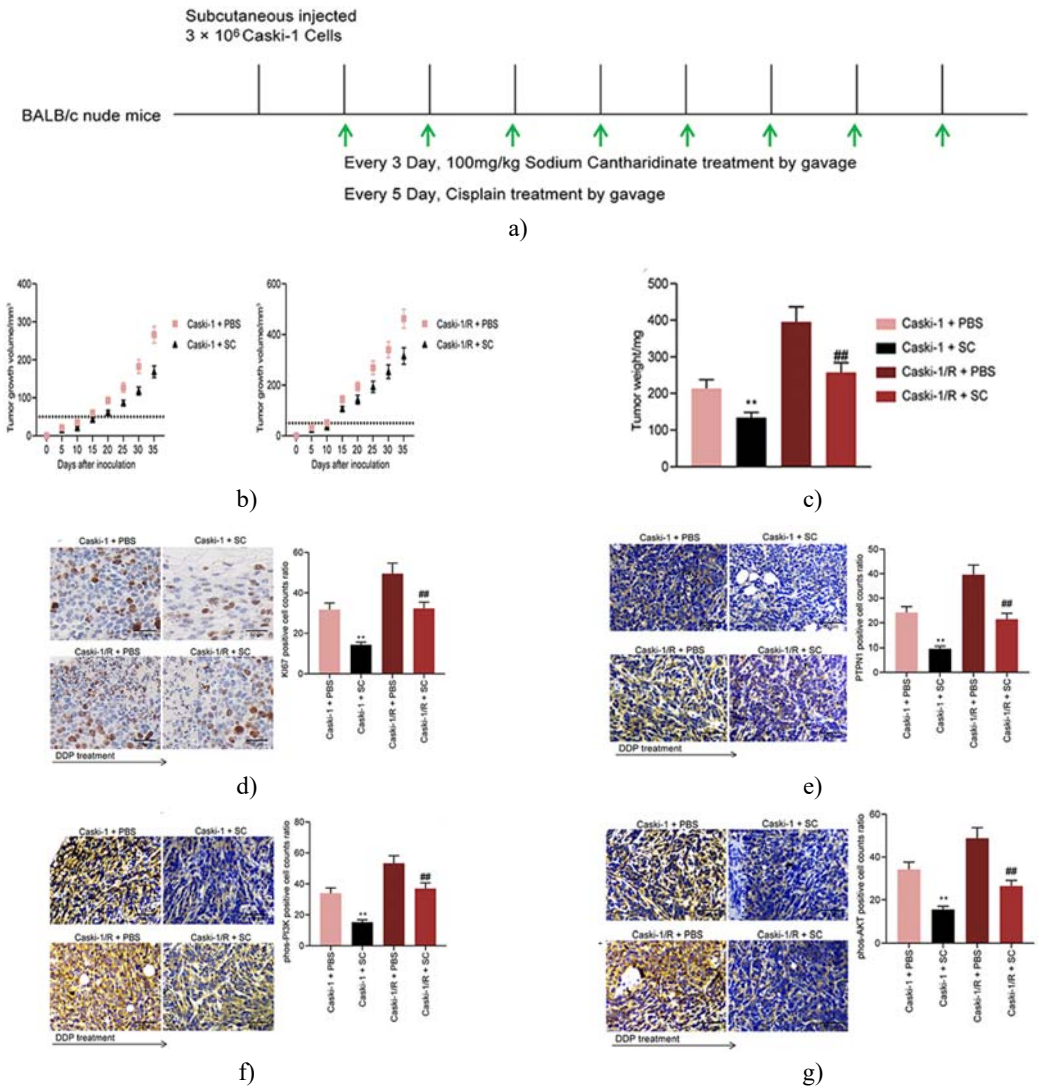

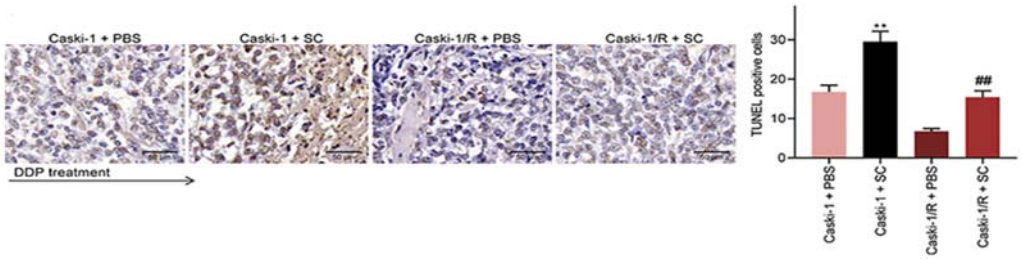

h)

Figure 7. SC suppresses tumor growth and chemoresistance of cervical cancer cells in vivo.
(a) Schematic representation of the experimental design.
(b) Tumor growth curves of xenografts over time.
(c) Final tumor weights.
(d–g) Immunohistochemical analysis of KI67 (d), PTPN1 (e), phosphorylated PI3K (F), and phosphorylated AKT1 (g) in tumor tissues.
(h) Apoptotic cell fraction detected by TUNEL staining.
Data are expressed as mean ± SD from three independent experiments (n = 6). Statistical comparisons were performed using one-way ANOVA (c–h) or two-way ANOVA (B) with Tukey's post hoc test. **$p < 0.01$ vs mice implanted with Caski-1 + PBS; ##$p < 0.01$ vs mice implanted with Caski-1/R + PBS.

Cisplatin (DDP) remains a cornerstone chemotherapeutic agent for multiple cancers, including bladder, head and neck, lung, ovarian, and testicular malignancies [16]. Nevertheless, the development of chemoresistance is a major factor limiting its effectiveness in cervical cancer (CC), often resulting in treatment failure, recurrence, and poor prognosis [17]. In the present study, we demonstrated that sodium cantharidinate (SC) not only inhibits CC cell proliferation but also significantly enhances DDP-induced cytotoxicity. Mechanistically, SC downregulated PTPN1 expression, and restoration of PTPN1 partially rescued cells from SC-induced chemosensitization. Our findings further confirmed that PTPN1 contributes to chemoresistance via activation of the PI3K/AKT signaling pathway.

Previous studies have highlighted the anticancer properties of SC in various tumor types, such as improving treatment outcomes and reducing toxicity in non-small-cell lung cancer [18], or promoting apoptosis in hepatocellular carcinoma via suppression of S100A3 [19]. In the current study, treatment of both parental and DDP-resistant CC cells with SC markedly reduced the expression of stem cell markers and the formation of tumor spheres. Co-treatment with DDP further decreased the IC50 values and increased apoptosis and LDH release, indicating that SC can effectively reverse chemoresistance. These observations align with prior reports that cantharidin derivatives enhance caspase-3 activity and apoptosis in bladder cancer cells [20].

Mechanistically, we identified PTPN1 as a direct target of SC. PTPN1 expression promoted PI3K/AKT pathway activation, which is well known to contribute to drug resistance in multiple cancers [21, 22]. Our in vitro experiments demonstrated that overexpression of PTPN1 reduced SC-induced apoptosis and cytotoxicity, highlighting the central role of this phosphatase in mediating chemoresistance. Dysregulation of the PI3K/AKT pathway is frequently implicated in tumor progression, and targeting this pathway in combination with chemotherapy may improve therapeutic outcomes [23, 24]. Activation of PI3K/AKT by Recilisib counteracted SC-mediated sensitization to DDP, confirming the involvement of this signaling axis.

These results provide a rationale for exploring SC as a therapeutic agent to overcome chemoresistance in CC. By targeting PTPN1 and attenuating PI3K/AKT signaling, SC can enhance the efficacy of DDP and potentially improve patient outcomes.

Conclusion

In summary, our study demonstrates that SC effectively inhibits the growth of Caski-1 and ME180 cervical cancer cells and sensitizes them to cisplatin treatment. This effect is mediated through suppression of PTPN1 expression and subsequent downregulation of the PI3K/AKT pathway. SC represents a promising pharmacological candidate for overcoming chemoresistance in CC. While further in vivo studies using additional cell lines such as ME180

are warranted, our data provide compelling evidence that SC may serve as an adjunct therapy to enhance cisplatin efficacy and combat drug resistance.

Acknowledgments: None

Conflict of Interest: None

Financial Support: None

Ethics Statement: None

References

1. Bray F, Ferlay J, Soerjomataram I, Siegel RL, Torre LA, Jemal A. Global cancer statistics 2018: GLOBOCAN estimates of incidence and mortality worldwide for 36 cancers in 185 countries. CA Cancer J Clin. 2018;68(6):394-424. doi:10.3322/caac.21492
2. Menderes G, Black J, Schwab CL, Santin AD. Immunotherapy and targeted therapy for cervical cancer: an update. Expert Rev Anticancer Ther. 2016;16(1):83-98. doi:10.1586/14737140.2016.1121108
3. Shen DW, Pouliot LM, Hall MD, Gottesman MM. Cisplatin resistance: a cellular self-defense mechanism resulting from multiple epigenetic and genetic changes. Pharmacol Rev. 2012;64(3):706-21. doi:10.1124/pr.111.005637
4. Zhu H, Luo H, Zhang W, Shen Z, Hu X, Zhu X. Molecular mechanisms of cisplatin resistance in cervical cancer. Drug Des Devel Ther. 2016;10:1885-95. doi:10.2147/DDDT.S106412
5. Yeh CB, Su CJ, Hwang JM, Chou MC. Therapeutic effects of cantharidin analogues without bridging ether oxygen on human hepatocellular carcinoma cells. Eur J Med Chem. 2010;45(9):3981-5. doi:10.1016/j.ejmech.2010.05.053
6. Deng LP, Dong J, Cai H, Wang W. Cantharidin as an antitumor agent: a retrospective review. Curr Med Chem. 2013;20(2):159-66. doi:10.2174/092986713804806711
7. Tao R, Sun WY, Yu DH, Qiu W, Yan WW, Ding YH, et al. Sodium cantharidinate induces HepG2 cell apoptosis through LC3 autophagy pathway. Oncol Rep. 2017;38(2):1233-9. doi:10.3892/or.2017.5779
8. Hale AJ, ter Steege E, den Hertog J. Recent advances in understanding the role of protein-tyrosine phosphatases in development and disease. Dev Biol. 2017;428(2):283-92. doi:10.1016/j.ydbio.2017.03.023
9. Lee H, Yi JS, Lawan A, Min KJ, Bennett AM. Mining the function of protein tyrosine phosphatases in health and disease. Semin Cell Dev Biol. 2015;37:66-72. doi:10.1016/j.semcdb.2014.09.021
10. Chen J, Zhao X, Yuan Y, Jing JJ. The expression patterns and the diagnostic/prognostic roles of PTPN family members in digestive tract cancers. Cancer Cell Int. 2020;20:238. doi:10.1186/s12935-020-01315-7
11. Liu H, Wu Y, Zhu S, Liang W, Liu Z, Liu Y, et al. PTP1B promotes cell proliferation and metastasis through activating src and ERK1/2 in non-small cell lung cancer. Cancer Lett. 2015;359(2):218-25. doi:10.1016/j.canlet.2015.01.020
12. Kuban-Jankowska A, Gorska-Ponikowska M, Sahu KK, Wozniak M. Docosahexaenoic acid inhibits PTP1B phosphatase and the viability of MCF-7 breast cancer cells. Nutrients. 2019;11(11):2554. doi:10.3390/nu11112554
13. Li Z, Hu C, Zhen Y, Pang B, Yi H, Chen X, et al. Pristimerin inhibits glioma progression by targeting AGO2 and PTPN1 expression via miR-542-5p. Biosci Rep. 2019;39(5):BSR20190003. doi:10.1042/BSR20190003
14. Chen Y, Tang J, Lu T, Liu F. CAPN1 promotes malignant behavior and erlotinib resistance mediated by phosphorylation of c-Met and PIK3R2 via degrading PTPN1 in lung adenocarcinoma. Thorac Cancer. 2020;11(7):1848-60. doi:10.1111/1759-7714.13465
15. Jin T, Li D, Yang T, Liu F, Kong J, Zhang L, et al. PTPN1 promotes the progression of glioma by activating the MAPK/ERK and PI3K/AKT pathways and is associated with poor patient survival. Oncol Rep. 2019;42(2):717-25. doi:10.3892/or.2019.7180
16. Dasari S, Tchounwou PB. Cisplatin in cancer therapy: molecular mechanisms of action. Eur J Pharmacol. 2014;740:364-78. doi:10.1016/j.ejphar.2014.07.025

17. Fang X, Zhong G, Wang Y, Lin Z, Lin R, Sun Y, et al. Low GAS5 expression may predict poor survival and cisplatin resistance in cervical cancer. Cell Death Dis. 2020;11(7):531. doi:10.1038/s41419-020-2735-2
18. Xiao Z, Wang C, Tan Z, Hu X, Chen Y, Li J, et al. Clinical efficacy and safety of sodium cantharidinate plus chemotherapy in non-small-cell lung cancer: a systematic review and meta-analysis of 38 randomized controlled trials. J Clin Pharm Ther. 2019;44(1):23-38. doi:10.1111/jcpt.12761
19. Tao R, Wang ZF, Qiu W, He YP, Yan WW, Sun WY, et al. Role of S100A3 in human hepatocellular carcinoma and the anticancer effect of sodium cantharidinate. Exp Ther Med. 2017;13(6):2812-8. doi:10.3892/etm.2017.4294
20. Zang GH, Li R, Zhou RS, Sun XJ, Liu Y, Zhang Y, et al. Effects of disodium cantharidinate on dendritic cells of patients with bladder carcinoma. Oncol Lett. 2018;15(2):2273-7. doi:10.3892/ol.2017.7589
21. Kostrzewa T, Styszko J, Gorska-Ponikowska M, Kuban-Jankowska A. Inhibitors of protein tyrosine phosphatase PTP1B with anticancer potential. Anticancer Res. 2019;39(7):3379-84. doi:10.21873/anticanres.13481
22. Yu M, Liu Z, Liu Y, Zhou H, Li H, Li X, et al. PTP1B markedly promotes breast cancer progression and is regulated by miR-193a-3p. FEBS J. 2019;286(6):1136-53. doi:10.1111/febs.14724
23. Bartholomeusz C, Gonzalez-Angulo AM. Targeting the PI3K signaling pathway in cancer therapy. Expert Opin Ther Targets. 2012;16(1):121-30. doi:10.1517/14728222.2011.644788
24. Amirani E, Hallajzadeh J, Asemi Z, Mansournia MA, Yousefi B. Effects of chitosan and oligochitosans on the phosphatidylinositol 3-kinase-AKT pathway in cancer therapy. Int J Biol Macromol. 2020;164:456-67. doi:10.1016/j.ijbiomac.2020.07.137